Atlantic Water intrusion triggers rapid retreat and regime change at previously stable Greenland glacier

Thomas R. Chudley
Byrd Polar and Climate Research Center, Ohio State University, Columbus, OH, USA
https://orcid.org/0000-0001-8547-1132

Ian M. Howat
Byrd Polar and Climate Research Center, Ohio State University, Columbus, OH, USA
School of Earth Sciences, Ohio State University, Columbus, OH, USA
https://orcid.org/0000-0002-8072-6260

Michalea D. King
Polar Science Center, University of Washington, Seattle, WA, USA
https://orcid.org/0000-0002-8138-4362

Adelaide Negrete
Byrd Polar and Climate Research Center, Ohio State University, Columbus, OH, USA

Correspondence: Tom Chudley (chudley.1@osu.edu)

Atlantic Water intrusion triggers rapid retreat and regime change at previously stable Greenland glacier

Chudley, T. R.[1]*, Howat, I. M.[1,2], King, M. D.[3], Negrete, A.[1]

[1] Byrd Polar and Climate Research Center, Ohio State University, Columbus, OH, USA
[2] School of Earth Sciences, Ohio State University, Columbus, OH, USA
[3] Polar Science Center, University of Washington, Seattle, WA, USA

Correspondence: Tom Chudley (chudley.1@osu.edu)

Abstract

Discharge from Greenland's marine-terminating glaciers contribute to half of all mass loss from the ice sheet, but the factors forcing their retreat are complex and contested. Here, we examine K.I.V Steenstrups Nordre Bræ ('Steenstrup'), which, between 2018—2021, retreated ~7 km, thinned by ~20%, doubled in ice discharge, and quadrupled in flow speed. This rate of acceleration is unprecedented amongst Greenland's glaciers, and now places Steenstrup in the top 10% of glaciers by contribution to Greenland's discharge. In contrast to expected behaviour from a shallow, grounded tidewater glacier, Steenstrup was insensitive to high surface temperatures that destabilised many regional glaciers in 2016, responding instead to an extreme anomaly in deeper Atlantic Water (AW) in 2018. Steenstrup's behaviour highlights that, as AW intrusions occur at increasingly shallow depths, even apparently long-term stable glaciers with high sills are vulnerable to sudden and rapid retreat.

1. Introduction

The Greenland Ice Sheet is currently the dominant contributor to global sea-level rise from the cryosphere, losing 222 ± 30 billion tonnes of ice per year between 2012 and 2017 (IMBIE Team, 2020). Between a half and two-thirds of this loss has been attributed to acceleration in the discharge from marine-terminating outlet glaciers since the 1990s (IMBIE Team, 2020; Mouginot *et al.* 2019, King *et al.* 2020), a process which is commonly understood to be initiated through interactions between the ocean and the glacier terminus (Catania *et al.* 2020). Understanding these interactions is a critical component of understanding future sea level contributions from the Greenland Ice Sheet.

Forcing at the ice-ocean interface is generally understood to occur via two primary mechanisms. First is the transport of warm, deep Atlantic Water (AW) through fjords to glacier calving fronts (Seale *et al.* 2011, Straneo and Heinbach, 2013, Slater *et al.* 2020), which, with heat transfer enabled by near-ice circulation and plumes (Slater *et al.* 2018, Fried *et al.*, 2015), initiate calving loss by submarine melt and undercutting of the ice front (Wood *et al.* 2018; 2021). The second is through warm surface waters, which can act to reduce ice melange stability (Walter *et al.* 2012; Cassotto *et al.* 2015; Moon *et al.* 2015; Bevan *et al.* 2019; Joughin *et al.* 2020; Fried *et al.* 2018), the backstress of which otherwise acts to inhibit calving (Burton *et al.* 2018, Todd *et al.* 2018;

Schlemm and Levermann, 2021). Both mechanisms have the potential to trigger rapid retreat in previously stable glaciers through positive feedbacks arising from retrograde bed slopes (Catania *et al.* 2018) and dynamic thinning (Felikson *et al.* 2017, Cassotto *et al.* 2019).

However, glaciers may exhibit highly heterogeneous responses to relatively uniform ocean forcing (King *et al.* 2020; Mouginot *et al.* 2019), even when termini are directly adjacent (e.g. McFadden *et al.* 2011, An *et al.* 2021, Carr *et al.* 2014). This variability has been attributed to fjord geometry (Wood *et al.* 2021, Millan *et al.* 2018), glacier geometry (Enderlin *et al.* 2013, Morlhigem *et al.* 2016, Felikson *et al.* 2017, Todd *et al.* 2018), subglacial hydrology (Bartholomaus *et al.* 2016), and the distribution of oceanographic currents (Seale *et al.* 2011; Walsh *et al.* 2012). None of these, however, can consistently explain spatial or temporal variability in outlet glaciers, suggesting that such variability is a complex combination of multiple conditions. For instance, some have argued that deep termini, susceptible to buoyant flexure and losing mass through full-thickness calving events, are controlled by seasonal (Moon *et al.* 2015) and inter-annual (Bevan *et al.* 2019) mélange variability, whilst shallow glaciers with displaying primarily small-magnitude serac failure have retreat driven primarily by subglacial melt (Fried *et al.* 2018; Catania *et al.* 2020). Meanwhile, others have suggested that the retreat of glaciers with deeper fjords and grounding lines are forced by AW intrusion, whilst shallow, well-grounded glaciers are protected by their proglacial bathymetry (Millan *et al.* 2018; Wood *et al.* 2021, Jakobsson *et al.* 2020). The former has been supported by glacier-scale studies of deep outlets such as Sermeq Kujalleq (Jakobshavn Isbræ) and Kangerlussuaq (Joughin *et al.* 2020, Bevan *et al.* 2019), which both conclude that retreat was initiated by the destabilisation of rigid winter mélange. Meanwhile, other studies have found deep outlets such as Zachariae Isstrøm (An *et al.* 2021) and Helheim (Straneo and Heimbach, 2013), to be forced primarily by AW. Todd *et al.* (2019) found Sermeq Kujalleq (Store Glacier) susceptible to both processes, destabilising entirely in response to either a doubling of frontal melt or a complete loss of mélange. This is problematic for larger-scale modelling exercises, which frequently choose only one mode of ice-ocean interaction to parameterise (Morlighem *et al.* 2019, Slater *et al.* 2020). Being able to better diagnose the controls on tidewater glacier vulnerability is important as many glaciers that contribute significantly to Greenland's cumulative discharge are less well studied than the few that dominate the literature (Mouginot *et al.* 2019).

This diverse attribution of forcing has typified Greenland's southeast sector. A dramatic increase in discharge from c. 2001 that extended as far as 69°N was attributed to AW (Seale *et al.* 2011; Straneo and Heinbach, 2013), corresponding with the latitudinal extent of the warm subtropical waters carried by the Irminger Current (Seal *et al.* 2011; Walsh *et al.* 2012). These retreating glaciers were typified by deep fjords (allowing AW access) and retrograde bedslopes (Millan *et al.* 2018). However, a more recent synchronised retreat in response to atmospheric warming began across the sector in 2016 (Liu *et al.* 2022), including at Kangerlussuaq (Bevan *et al.* 2019; Brough *et al.* 2019). Studies of ocean reanalysis data concluded that this response was not due to AW, which experienced no anomaly in 2016 (Bevan *et al.* 2019; Liu *et al.* 2022). Instead, it was proposed that the retreats occurred in response to either (i) atmospheric forcing leading to a high cumulative meltwater input, resulting in increased submarine melt at the front (Liu *et al.* 2022); or (ii) surface-level ocean forcing resulting in a loss of winter rigid mélange, leading to increased calving (Bevan *et al.* 2019). Once again, understanding controls on tidewater glacier vulnerability is necessary for both identifying the climate and ocean conditions that lead to past retreat and for predicting future change.

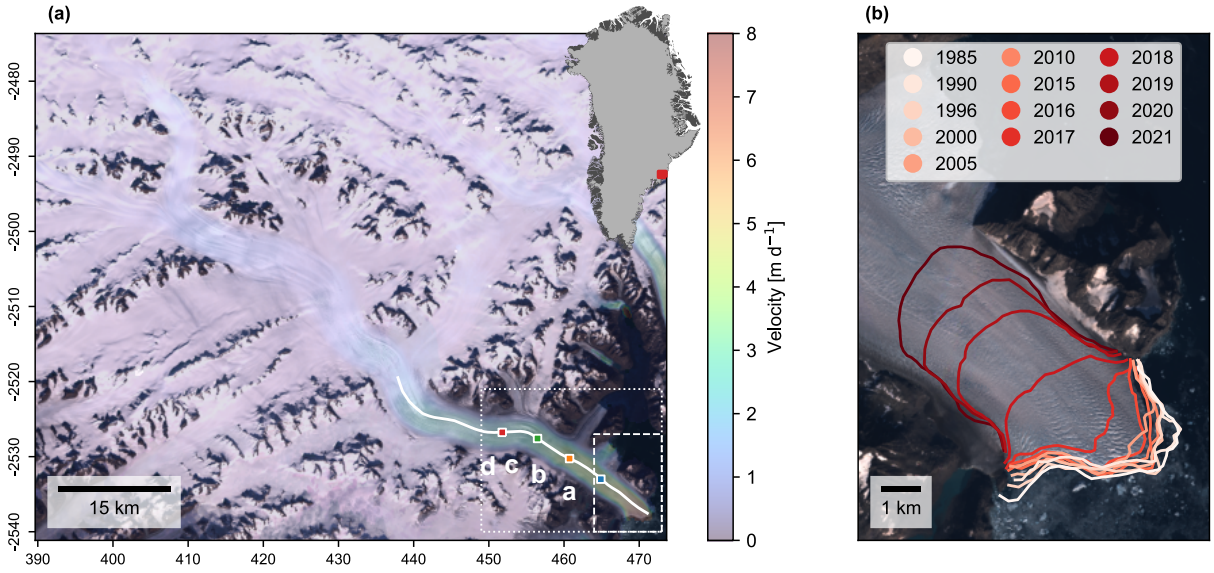

Figure 1: *(a) Location and speed of KIV Steenstrup Nordre Bræ. Colour scale indicates the mean 2016 velocity from ITS_LIVE velocity pairs. Coloured squares a-d indicate locations used to sample velocity time-series in fig. 2, whilst white line marks centreline used to derive profiles in fig. 3. Dotted box marks extent of fig. 4 and dashed box marks extent of panel b. Background is a composite of median Sentinel-2 RGB pixel values May–October 2016. Coordinates in unit kilometres of NSIDC Polar Stereographic North. Inset shows location of Steenstrup within Greenland. (b) Changing front position of Steenstrup since 2016, identified using GEEDiT (Lea* et al. *2019).*

Here, we examine recent changes at K.I.V Steenstrups Nordre Bræ (66.53 °N, 34.57 °W; fig. 1a; hereafter Steenstrup), an outlet glacier of the southeast Greenland Ice Sheet that exhibited long-term stability until dramatic destabilisation in 2018. We use observations and reanalysis products to outline the extent of change and understand the underlying mechanisms, identifying the sensitivities of the glacier to forcing out and outlining how this changes through time.

2. Results

2.1. Temporal changes at Steenstrup

Prior to 2018, Steenstrup's calving front was stable throughout the late 20th and early 21st century, with an average 2015 front position only ~200 metres from the average 1985 front position (fig. 2a). The average speed at the calving front was ~7 m d^{-1} (~2.5 km a^{-1}) (fig. 1a), with a discharge of 3.34 Gt a^{-1} in 2016, putting it in the 82nd percentile of glaciers by contribution to Greenland's discharge. Seasonal variability was low, with a standard deviation of seasonal front position of 155 m. Most years exhibited a negligible seasonal advance or retreat, barring a few exceptions (2002, 2009, 2010, 2014, 2016) which displayed ~0.8-1.0 km of retreat beginning in June but recovering, often overwinter but always within ~2 years. For instance, between early June and late October 2016 in 2016, Steenstrup's calving front retreated by just over 1 km. The front remained relatively stable through the winter, retreating by only another 80 m until the first observation of 2017 (2017-02-19), by which point the glacier was advancing, ending the season ~0.2 km advanced from where it began.

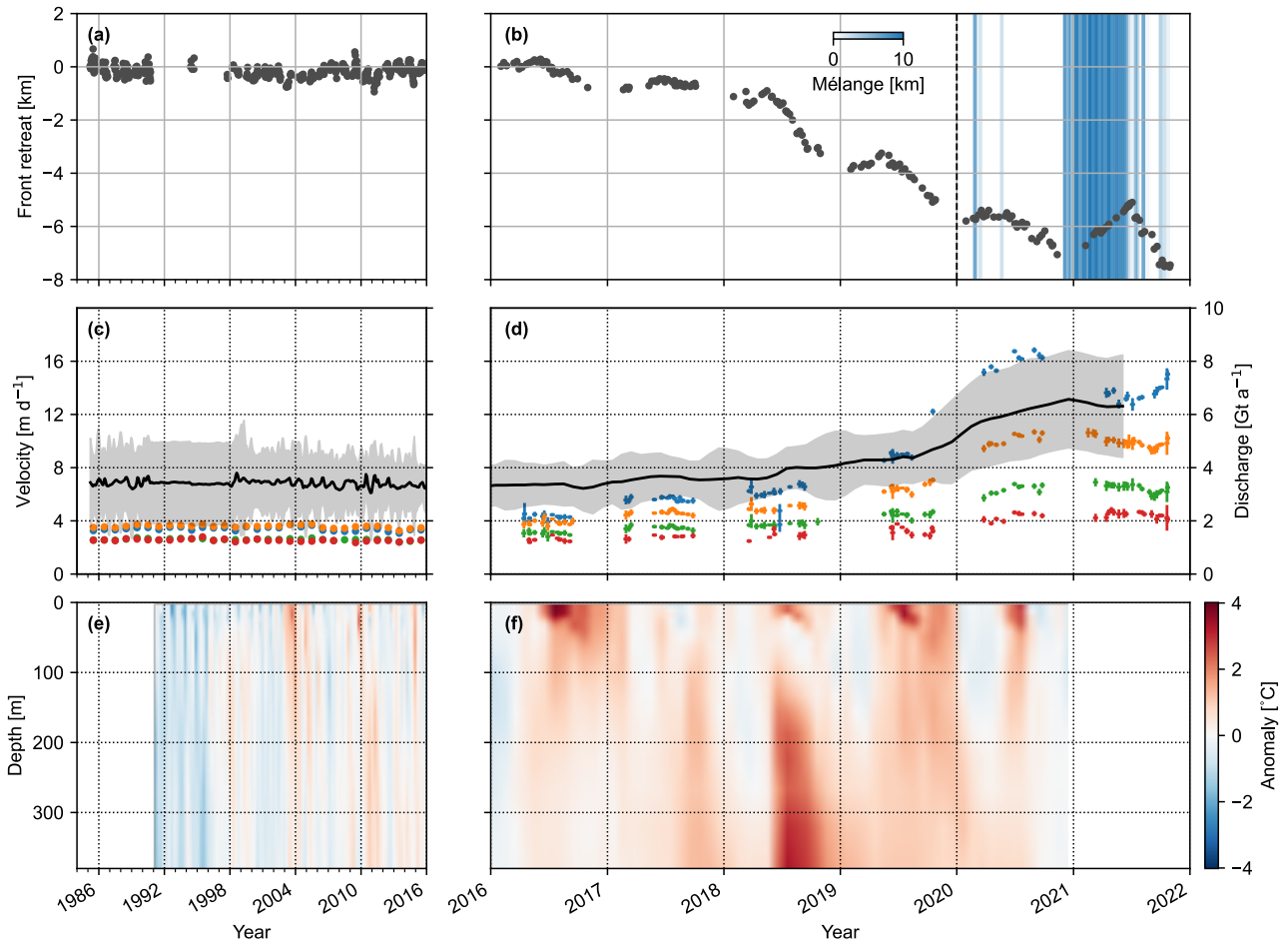

Figure 2: *Front position between (a) 1985 and 2015 and (b) 2016 and 2022, with blue shading denoting the extent of rigid mélange between 2020 and 2021 (a zoomed 2020-2021 version of panel (b) is shown as fig. S1). Black dashed line marks beginning of the mélange record (January 2020). Discharge (black curve with shading as 2σ uncertainty) and annual velocity (colored points with errorbars) between (c) 1985 and 2015 and (d) 2016 and 2022. Point colours refer to points in Fig 1a. Mean ocean temperature anomaly for the CE1 sample zone (fig. S5) between (e) 1992 and 2015 and (f) 2016 and 2021.*

In contrast, 2018 saw more significant and sustained retreats. This began in mid-May, totalling 2.4 km by the last observation in late October, with a further 600 m of retreat occurring over winter. This pattern repeated in 2019, retreating 1750 m between mid-May and the final observation (26 October), and a further 800 m through the winter. An additional ~1600 m of retreat occurred between early May and November, 2020, but, unlike the previous three years, the front re-advanced overwinter, by ~340 m. This notable advance continued into 2021, where the terminus maxima (observed on 4th July) was 262 m beyond the 2020 maximum. However, this advance was reversed by a significant late-summer retreat, ultimately losing ~380 m at the end of the season compared to the previous year. In total, Steenstrup retreated 6.6 km between 2018 and 2021.

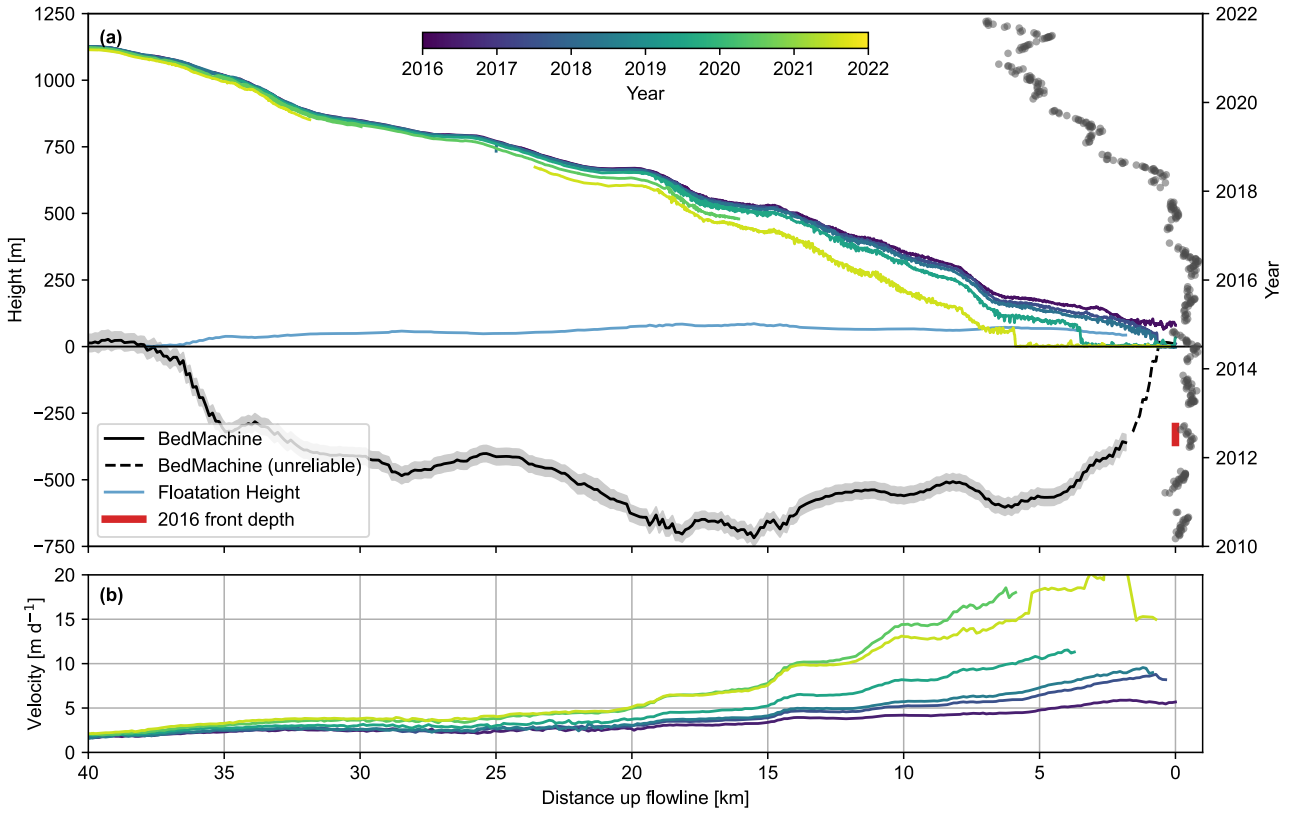

Figure 3: *(a) Surface (ArcticDEM strips) and bed elevation (BedMachine v4) along the profile shown in Fig. 1a. Blue line shows the floatation height of the ice column. Grey dots mark terminus positions through time. Red bar marks the vertical range of the 2016 terminus depth from Oceans Melting Greenland Multi Beam Echo Sounder data (Oceans Melting Greenland, 2019). Note that the front 1.8 km of the BedMachine data, denoted with a dashed line, is determined to be unreliable based on OMG data (see supplementary text). (b) Annual speed profiles from ITS_LIVE velocity data along the profile shown in Fig. 1a.*

The retreat of the calving front was matched by an associated increase in glacier speed. Flow speed at all points along the flowline showed little change in the thirty years of observations before 2016 (Fig 2b-c). Speed increased at all points between 2016 and 2020, reaching a maximum of 16.8 m d^{-1} at the frontmost sampling point in August 2020 (an increase of more than 270%). However, alongside the significant advance in frontal position that occurred up until July 2021, the speed at all points was greatly reduced, declining to ~12.8 m d^{-1} at the frontmost point by early July. At the point closest to the glacier front, acceleration occurred coincident with the retreat of the glacier calving front and continued for the rest of the year, reaching a maximum of 15.0 m d^{-1} in the last observation of the year (2021-10-22). However, it took time for this acceleration to propagate inland, with the two points further inland not accelerating until late August / early September, whilst the point furthest from the terminus showed no clear late-season acceleration. The increase in ice flow velocity resulted in a near doubling in the rate of ice discharge by 2021, reaching 6.37 Gt a^{-1}, placing Steenstrup in the 93rd percentile of Greenland's outlet glaciers by contribution to total discharge (up from 3.34 Gt a^{-1} and 82nd percentile in 2016).

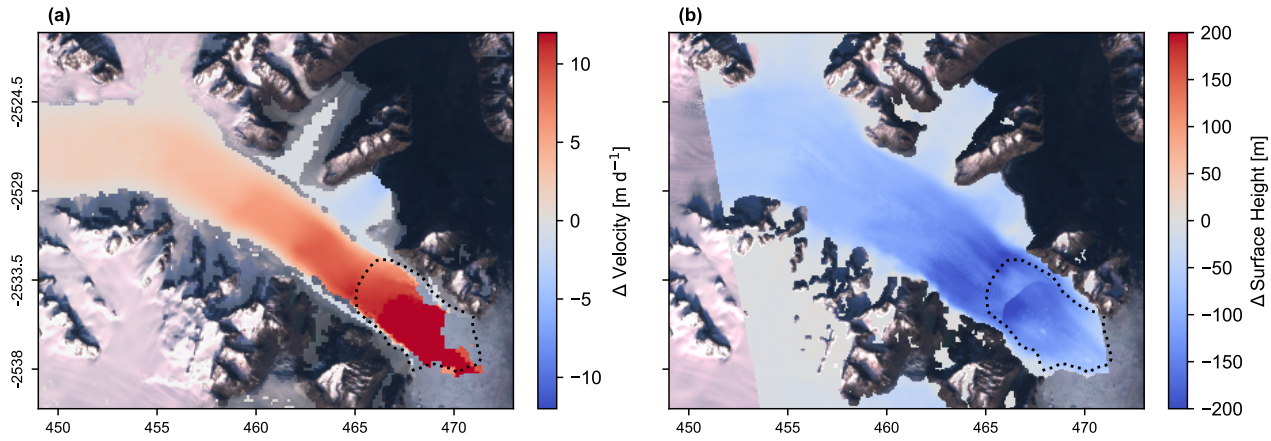

Figure 4: *Spatial extent of change. (a) Difference between the weighted mean average of 2021 and 2016 ITS_LIVE velocity pairs. Colours are translucent where change is not significant. (b) DEM difference between ArcticDEM strips captured on 2016-03-27 and 2021-07-31. Dotted lines mark terminus positions on 2016-09-28 and 2021-10-29. Coordinates in unit kilometres of NSIDC Polar Stereographic North.*

Sampling annual velocity mosaics along the flowline (fig 3b) provides further information about the temporal extent of speed increases. Statistically significant increases in speed are visible up to 40 km inland, where there was a progressive, year-on-year increase in speed from 1.7 m d^{-1} in 2016 to 2.1 m d^{-1} in 2021 (a 24% increase). On average, speed increased over 100% within 19 km of the 2016 front position, over 50% within 27 km, and over 20% within 40 km. This acceleration was limited to the main glacier trunk and did not extend to either of the northeast calving distributaries. Indeed, both distributaries exhibited statistically significant slowdowns, the northernmost distributary from ~0.5 m d^{-1} to ~0.2 m d^{-1}, and the southernmost from ~4.4 m d^{-1} to ~0.9 m d^{1} (fig. 4a). This contrasting behaviour between the main outlet and distributaries was associated with a significant shift in the median moraine of the northernmost distributary as flow was captured by the main outlet (fig. S2).

The retreat and acceleration of Steenstrup was also associated with a significant reduction in surface elevation far greater than could be attributed to increased surface melting and, therefore, is attributed to ice thinning under increased along-flow strain rates (i.e. dynamic thinning). Between 2016 and 2018, the glacier thinned by ~10 - 20 m a^{-1} within ~6 km of the 2016 front, with the rate of thinning decreasing to 1-2 m a^{-1} by 20 km inland (fig. 3a). However, after 2018, thinning accelerated and propagated inland rapidly. Between 8 and 10 km upglacier of the 2016 terminus, losses approached 50 m a^{-1} between 2018 and 2021. By 2021, a combination of surface elevation loss and retreat along a retrograde bedslope resulted in ~1 km of the tongue being at or near flotation by 2021, as indicated by the ice surface height relative to flotation (fig. 3a). Total elevation losses exceeded 200 m between 2016 and 2020 (fig. 4b). Surface losses also occurred in the distributaries between 2016–2021: up to 40 m at the terminus of the northern distributary and 60 m at the southern distributary

2.2. Temperature Forcing

CMEMS reanalysis data (fig. 2e-f) indicate that positive anomalies in surface waters (relative to the 1992-2020 monthly mean) occurred frequently from ~2000 onwards. These increases were typically associated with seasonal retreats in front position (e.g., 2003, 2009, 2010, and 2014) -

most notably in 2016, when surface temperature anomalies exceeded +3.8 ˚C of the 1992-2020 mean in July. However, in these cases, retreat was ephemeral and readvanced over the subsequent winter. We note that the anomalies in 2016 upper ocean temperatures are not reflected in air temperatures from the two nearest weather stations (fig. S3), which further do not show any significant correlation with glacier terminus behaviour.

The significant retreat period that began in 2018 was synchronous with an exceptionally warm and thick temperature anomaly that reached to within 100 m below the sea surface. At 380 m (the deepest level that reanalysis data covers in the sample region), this anomaly reached a maximum of +3.3 ˚C in July 2018 (the second-highest annual maxima, in October 2017, was only +1.3 ˚C). At 186 m (the reanalysis depth above which water could overtop the proglacial sill), the July 2018 anomaly was +2.4 ˚C.

3. Discussion

3.1. Rate and extent of destabilisation

Both this study and others indicate that Steenstrup has been stable on at least a decadal time scale prior to 2018. Data from the Landsat record (fig. 2a-b) is indicative of stability with very little seasonal variation going back to at least the 1980s. The front position further remains broadly the same in 1966 declassified satellite imagery, with Cooper *et al.* (2022) reporting a negligible advance rate of 13.3 m a^{-1} between 1966 and 1985. The glacier front position further appears constant in 1938-1942 cartographic records (US Army Map Service, 1952). The stability of this frontal position is also supported by the presence of a push moraine only 200 m from the 2016 front position (fig. S4a), which Batchelor *et al.* (2019) attribute to a 20th-century regime. It is likely that any significant advance beyond this was limited by a subsequent increase in exposed calving face to the ocean, implying the formation of a floating free tongue, whilst any retreat forcing was stabilised by the front position on a ridge (e.g. Morlhigem *et al.* 2016, Millan *et al.* 2018). Regardless, it is notable that there was no significant precursor activity before the destabilisation that occurred in 2018, suggesting a sudden, external forcing.

The destabilisation that occurred between 2018-2021 was considerable in magnitude and extent. Steenstrup retreated ~7 km, thinned at a rate of nearly 50 m a^{-1}, quadrupled in speed, and doubled in discharge. Whilst retreat rates in excess of a kilometre per year have precedent across tidewater glaciers (e.g. Hill *et al.* 2018), this rate of retreat is still extreme, with most glaciers exhibiting retreat rates of <200 m a^{-1} (Bunce *et al.* 2018). Meanwhile, the dynamic thinning rate exceeds many significant glacier retreats, such as Kangerlussuaq (Kherl *et al.* 2017, Brough *et al.* 2019), and matches that of Jakobshavn during the early 2000s (Howat *et al.* 2007, Holland *et al.* 2008, Khazendar *et al.* 2019). Although absolute velocity is still lower, the relative acceleration - with up to a quadrupling of speeds within five years - is, to our knowledge, unprecedented, outweighing many of the largest events seen on the ice sheet (Moon *et al.* 2012), including Jakobshavn in the early 2000s, which saw an approximate doubling in velocity in five years (Howat *et al.* 2007). The short-term doubling of discharge is likewise unprecedented and only exceeded by Harald Moltke Bræ, which ~tripled its annual discharge within the span of a decade (King et al. 2020), but this is explained by it entering a surge phase (Müller *et al.* 2021). Hence, recent events at Steenstrup are comparable to, or exceed, the largest instances of tidewater glacier change across the Greenland Ice Sheet. Moon *et al.* (2012) suggested that rapid and large

destabilisation may be limited to only a few glaciers. The case of Steenstrup, however, suggests that other, apparently stable, glaciers may still be primed to retreat under ever more extreme forcing (Christian *et al.* 2022).

3.2. Forcing mechanisms

Prior studies have attributed retreat of southeastern sector tidewater glaciers since 2016 to two mechanisms: (i) Bevan et al. (2019) attributed the retreat of Kangerlussuaq to warm surface waters that prohibited the development of a rigid mélange in the winters of 2016/17 and 2017/18, leading to a loss of back stress and a subsequent increase in discharge; and (ii) in a broader sector-scale study, Liu et al. (2022) identified atmospheric forcing as the primary cause, with summers of high cumulative meltwater, and thus subglacial discharge, driving retreat via higher rates of terminus melt (e.g. Fried et al., 2018). However, both anomalous climate events - and the subsequent responses across the sector - occurred in 2016. Although Steenstrup saw a seasonal retreat in 2016, this was not as dramatic as at other glaciers, and commensurate with its historical response to other years with warm near-surface temperatures, including 2002, 2009, 2010, and 2014 (fig. 2). The recovery exhibited in 2017 indicated that Steenstrup was on a trajectory to recover its front position in line with previous seasonal retreats. Hence, Steenstrup did not share the extreme retreat response that was observed across the sector, despite the fact that relatively shallow, well-grounded glaciers such as Steenstrup have been hypothesised to be vulnerable to such events (e.g. Fried et al. 2018).

Insensitivity to near-surface water temperatures is consistent with the historical lack of mélange at Steenstrup. The satellite record shows that, prior to the 2018 retreat, only a small amount of mélange was observed in a small embayment on the southwest side of the terminus. This melange contacted land on only one side and therefore would not have provided significant backstress. The reason behind a lack of sensitivity to enhanced subglacial discharge remains less obvious. Liu et al. (2022) found no significant difference in runoff anomaly between glaciers that retreated in 2016 and those that did not, suggesting that high runoff alone is not sufficient alone to induce retreat. We suggest that the geometry of Steenstrup, with a confined and narrow trunk tens of kilometres long and ~100 km from the ice sheet proper, limits the availability of surface meltwater. This consequently limits the rate and magnitude of subglacial meltwater discharge from the terminus, and hence the ability for surface melt to induce terminus melt. Additionally, the two distributaries near the front may provide alternative outlets for subglacially routed meltwater. In either case, another forcing mechanism is necessary to explain Steenstrup's retreat.

Unstable retreat of Steenstrup began in 2018, with rates reaching kilometres per year between 2018 and 2021. This event was associated with anomalously warm waters beneath ~100 m and not near-surface waters (fig 2b). This suggests that Steenstrup's retreat was primarily initiated by submarine melt and undercutting forced by deep, warm AW (Seale et al. 2011, Straneo and Heinbach, 2013, Slater et al. 2020). The vulnerability of Steenstrup, which was relatively shallow and well-grounded at the ice front, to AW rather than near-surface water temperatures contrasts with expectations that AW is most effective at initiating retreat in shallow, well-grounded glaciers (Fried et al. 2018, Wood et al. 2021). Indeed, Wood et al. (2021) identify Steenstrup as a stable 'calving ridge' glacier, raised above the level of AW by a sill and having only a small floating section. It is of note, however, that this interpretation may be skewed by the poor BedMachine topographic reconstruction at this point (see supplementary text). Manually inspecting Oceans Melting Greenland Multi Beam Echo Sounder (OMG MBES) data (Oceans Melting Greenland,

2019) reveals that the depth at the calving front lies in the range ~300-360 m and the lower limit of the proglacial sill ~180 m (fig S3a). AW along the East Greenland Shelf primarily occurs beneath depths of ~250 m (Sutherland *et al.* 2013), above which cold and fresh polar water dominates. However, warm modes exist whereby AW can be present throughout the water column (Sutherland *et al.* 2013) and driven onto the coastal shelf (Jackson *et al.* 2014, Håvik and Våge, 2018). We suggest that 2018 is representative of a particularly extreme warm mode (also identified in observational data by Snow *et al.* 2021) sufficient to incorporate an anomalous amount of AW high into the water column at Kangerlussuaq Fjord (Fig. S6), which was then carried south across the coastal shelf as part of the East Greenland Coastal Current (Sutherland and Pickart, 2008; Håvik and Våge, 2018). The resultant anomaly in 2018 ocean temperatures extends to ~100 m in depth (fig 2b), far exceeding the ~180 m sill depth at Steenstrup. This is likely the first time that significant AW had been transported to the front of Steenstrup in at least the past several decades. AW presence across the shallow coastal shelf in front of Steenstrup (maximum depths of ~400 m in the sample zone) is rare compared to in front of Sermerlik and Kangerlussuaq Fjords, which have deep canyons to aid AW transfer (Sutherland *et al.* 2013; fig. S5). This is evident when comparing temperature anomaly data between the sites (figs. S5, S6). Although the warm 2018 is visible in thermal forcing data at all locations, only in front of Steenstrup is it anomalous (fig. S6), suggesting that 2018 is a particularly extreme AW intrusion that could access even the shallowest sections of the coastal shelf. Increasing warming of waters around Greenland since the mid-1990s (Straneo and Heinbach, 2013) may result in increasingly common AW access to marine-terminating glaciers thought to be protected by shallow shelves and sills. However, predicting which are vulnerable may be challenging in light of the poor reconstruction of terminus geometry in Greenland-wide datasets.

3.3. Transition to mélange-dominated regime

Following destabilisation, Steenstrup retreated at a rapid rate (~2 km a^{-1}) between 2018 and 2020. This retreat occurred down a retrograde bedslipe (fig 3a), inducing unstable retreat until the front retreated to another high in the bed and stabilised in 2021. Following this retreat, and unlike its behaviour prior to 2016, Steenstrup has displayed seasonal variability in terminus position, advancing significantly in the 2020/21 winter before retreating in summer 2021. This advance/retreat pattern is similar to the 'type b' glacier terminus behaviour described by Fried et al. (2018), retreating between ~June-September and advancing between ~September-June, and is attributed to the seasonal formation and breakup of mélange. This interpretation is supported by the mélange extent data (fig. 2b), which indicates that mélange was extensive in the 2020/21 winter but absent in 2019/20, and further supported by annual velocity mosaics, which incorporate fast-flowing (>16 m d^{-1}) mélange in the 2021 mosaic but not in previous years. We suggest that by the 2020/21 winter, the retreat of the terminus ~6 km from fjord edge enabled mélange to form fast to the fjord margins, resulting in great enough backstress on the glacier front to influence calving rate (e.g. Todd and Christoffersen, 2014). This was aided by the glacier thinning sufficiently that the terminus 1 km from the front was at or near floatation (fig. 3b). This meant that the balance of stresses acting on the glacier terminus were more sensitive to mélange backstress in the absence of reduced basal traction, modulating the new seasonal dynamic behaviour that emerged in 2021. It is of note that this transition is the opposite of that suggested by Sakakibara and Sugiyama (2018), who relate deep fjords to a lower seasonality of behaviour, as warm AW can intrude into fjords all year. Our evidence suggests that the presence/strength of a mélange may be more important in defining seasonal behaviour than fjord depth or AW availability.

3.4. Steenstrup's future

The ongoing retreat of Steenstrup slowed in 2021, likely due to a combination of reaching a section of prograde bedslope (fig 3b), reduction in driving stress due to rapid dynamic thinning, and the development of a rigid proglacial mélange that provided sufficient backstress to slow calving (section 3.3). However, the glacier is by no means stable. With velocities quadrupled since 2016, Steenstrup is likely far out of balance. Ice flow is confined to relatively narrow valleys and catchments until connecting to the ice sheet over 100 km upstream (fig. 1a): as such, diffusive acceleration and thinning are concentrated in the trunk, increasing rates of dynamic thinning relative to less confined glaciers (Moon et al. 2012). In this sense, the upstream response to retreat at Steenstrup is similar to Alaskan tidewater glaciers, such as Columbia Glacier (Walter *et al.* 2010), with a lack of influx resulting in hundreds of metres of thinning extending far upstream in a matter of years (fig. 4b). Rapid thinning is resolvable tens of kilometres inland (fig. 3b) and will likely continue in the medium term. This imbalance in discharge will likely persist due to a transition to a deeper terminus that is at or near floatation (fig. 3b). This has been suggested to enhance tabular calving driven by full-thickness fracture (Carr *et al.* 2013, Fried et al. 2018) rather than smaller, sub-aerial calving events, a transition that has been reported to occur at Columbia (Walter *et al.* 2010) and Bowdoin Glaciers (van Dongen *et al.* 2021). We suggest that these factors make the 2021 terminus position untenable in the medium term, even accounting for the current position on a short stretch of prograde bedslope (fig. 3b).

Once the terminus has retreated past the 2021 sill, the next ~8 km of retreat will be influenced by the collapse of the two tidewater distributaries, which are already thinning rapidly (fig. 4b). As these areas are also decelerating (fig. 4a), we suggest that this is not due to dynamic thinning but instead due to decreasing influx resulting from flow capture by the main trunk (fig. S2). Once the main terminus retreats past their input, the distributaries will rapidly disintegrate due to submarine melt and calving. However, their collapse will once again restrict the ability of a rigid mélange to form (due to a lack of fjord margins on the northeast side), enhancing calving rates and enabling ongoing retreat. According to BedMachine v4 (which may be poor at Steenstrup - see supplementary text), retrograde bedslopes continue to occur, with some rises that may or may not stall retreat (Robel *et al.* 2022), until approximately 20 km from the 2016 calving front. The extent to which the glacier stabilises or not between this point and when the bed reaches sea level (35 km inland) will be controlled by the full extent of dynamic thinning and ocean forcing.

With retrograde bed slopes above its current front position, imminent destabilisation, loss of distributaries, and continued dynamic thinning all indicate further, rapid retreat. However, the relative influence of atmospheric and oceanic forcing may modify the rate of response, especially at prograde bedrock rises. As identified above, Steenstrup's seasonal behaviour in 2021 suggests a new sensitivity to mélange variability. As a result, Steenstrup may now be newly vulnerable to warm anomalies in ocean surface temperature, as occurred in 2016 and was experienced by glaciers across the sector (Liu et al. 2022; Bevan *et al.* 2019). Meanwhile, the terminus will continue to be sensitive to warm AW instructions, especially if the collapse of the two northeastern distributaries provide new pathways for AW entry through the deeper northern fjord (fig. S4b). The future sensitivity of the glacier to surface melt and resultant subglacial discharge is less clear. However, a quadrupling in velocity may result in an increase in subglacial melt generated via frictional heating at the bed, whilst the increased positive surface strain rates in accelerating zones may provide new pathways for water to reach the bed through crevasses. As a

result, the changes occurring at Steenstrup may make it more vulnerable to a range of tidewater glacier retreat mechanisms.

4. Implications

Steenstrup provides a unique example of significant short-term glacier change that has occurred entirely within a period of intense observational study from various Earth observation instruments. Occurring without resolvable precursor activity, the destabilisation of Steenstrup from 2018 onwards marks one of the most significant rapid responses of a tidewater glacier, particularly from a glacier previously thought to be stable and insensitive to ocean forcing. The various responses to forcing exhibited between 2016 and 2021 prove instructive in verifying theories of ice-ocean sensitivity and highlight the ability of a tidewater glacier to transition between sensitivity to warm AW, warm surface temperatures (via mélange), and enhanced surface melt. Relative to retreats of other major outlet glaciers like Jakobshavn Isbrae and Kangerdlugssuaq, thinning and acceleration propagating inland from the ice front were amplified by Steenstrup's more confined geometry. Already possibly the highest relative increase in glacier speed observed amongst fast-moving tidewater glaciers in Greenland, significant change can be expected to continue into the coming years and decades. This makes Steenstrup a priority for ongoing observation as well as a good candidate for numerical modelling experiments: providing both the opportunity to test the ability of models to replicate complex changes and forcings, and to provide future projections that will be falsifiable on a timescale of years.

Model reanalysis presented here and elsewhere (e.g. Wood *et al.* 2021) show that AW around the GrIS is becoming progressively warmer in recent decades (Straneo and Heinbach, 2013), providing increasing opportunities for warm waters to penetrate to the front of marine-terminating glaciers that are relatively more protected from incursions by proglacial bathymetry (Christian *et al.* 2022). Steenstrup has shown that the stability of glaciers is hard to predict using our current knowledge of smaller, stable, and data-sparse glaciers, especially given the apparently poor reconstruction of the geometry of the ice-ocean interface at Steenstrup and elsewhere. There may be many more well-grounded and mélange-deficient glaciers that, whilst resistant to warm surface waters and subglacial discharge, are primed to retreat and increase their contribution to total GrIS discharge in the face of increasing AW incursion.

5. Methods

5.1. Calving front positions

Calving front positions were manually digitised along the centreline between 1985 and 2021 using Landsat 4 - 8 and ASTER data following Walsh *et al.* (2012).

5.2. Glacier velocity

We track the change in speed of Steenstrup with both scene-pair velocities (to construct time-series) and annual velocity maps (to assess spatial change). To do this, we make use of ITS_LIVE velocity data (Gardner et al., 2018, 2021). Between 1985 and 2015, we visualised annual mosaics of velocity provided by the ITS_LIVE project (Fig. 2c). Beyond 2016 (Fig. 2b), we download all available image pairs covering Steenstrup between 2016 and 2021 with >1% data coverage.

To present a time series (Fig. 2b) ITS_LIVE velocity pairs are sampled at locations between 6 km and 23 km along the flowline from the 2016 calving front (Table S1). We use 2016 as our pre-retreat standard across all observed variables as in 2017 the glacier displayed a retreated terminus and slightly enhanced velocity relative to 1985-2016 norm (fig. 2) due to the impact of warm surface water in 2016 that the glacier has historically recovered from within two years (section 2.1). We sample a 1 km × 1 km box centred on the point, presenting the median speed and error of the sample zone where coverage is greater than 70%.

As updated annual mosaics between 2019-2021 were not available at the time of writing, we calculated our own annual mosaics to produce difference maps between 2016 and 2021 for visualisation (Fig. 3b, 4a). From the provided speed (x) and error (σ) values, we calculate the weighted mean ($\bar{x}$) as:

$$\bar{x} = \frac{\sum x/\sigma^2}{\sum 1/\sigma^2},$$

and the weighted standard error as:

$$\bar{\sigma} = \sqrt{\frac{1}{\sum 1/\sigma^2}}.$$

A two-tailed unpaired *t*-test is used to assess whether differences between the mosaic pixels are significant (Fig. 4a).

5.3. Mélange presence

Melange velocities for are derived continuous 6-day periods throughout 2020 and 2021 from SAR imagery acquired in the interferometric wide swath (IW) mode from the Sentinel-1 A and B. Velocity maps over rigid mélange-occupied regions of the fjord and surrounding margin are processed following GrIMP workflows (Joughin *et al.* 2021), which measure 6-day displacements of features in image pairs by cross-correlating small (km-scale) image patches. Here, only the extent of rigid mélange is measured, or regions of icebergs and sea ice that can be tracked from one image to the next. By contrast, the mapping algorithm fails if the mélange is non-rigid, or such that the individual constituents of the mélange move more randomly relative to each other. When present, the extent of rigid mélange is derived by comparing the distance between the outer limit of rigid mélange areas, to the contemporaneous Steenstrup terminus position, which is manually traced at the same 6-day temporal resolution. Thus, in addition to understanding whether or not rigid mélange is present adjacent to the terminus at a given time step, mélange extent provides a metric to evaluate potential relative back force at the calving front.

5.4. Discharge

Monthly ice discharge from 1985 through 2021 is calculated through an upstream flux gate, oriented perpendicular to ice flow, across the width of Steenstrup Glacier following methods outlined in King *et al*. (2020). Original discharge estimates from that study are updated to reflect the release of new bathymetry estimates from Bed Machine Version 4 and appended through 2021 using recent ArcticDEM surface elevation data and GrIMP monthly InSAR ice velocity products.

5.5. Topographic Analysis

5.5.1. DEM Differencing

To assess elevation change over the period of interest, we use 2 m ArcticDEM strips (Porter *et al.* 2018). From the archive, we manually identify high-quality strips between 2016–2012 (Table S2), coregistering the strips to the 2016 DEM following the method of Nuth and Kääb (2011).

To explore the potential for floatation at the calving front, we estimate the theoretical floatation thickness (H_f) based on basal topography extracted from BedMachine v4 (Morlighem *et al.* 2017; Morlighem *et al.* 2021) as

$$H_f = -h_b \frac{\rho_w}{\rho_i},$$

where *H_b* is the bed depth, *H_a* is the thickness of the firn-air column, and ρ_i and ρ_w , are the densities of ice and water (assigned 917 and 1027 kg m^{-3}) respectively.

5.6. Oceanography data

5.6.1. Temperature Data

Following Bevan *et al.* (2021), we extract ocean potential temperatures from 1991-2020 from the Copernicus Marine Environment Monitoring Service (CMEMS) Arctic Ocean Physics Reanalysis monthly mean data (Copernicus Marine Environment Monitoring Service, 2021). We calculated monthly anomalies in the potential temperatures over the continental shelf in front of KJV Steenstrup (fig. 2b). Here, we use sampling zones matching Wood *et al.* (2021) - specifically zone CE1 (fig. S5).

For comparison, we present 2 m air temperature data (fig. S3), downloaded from the Danish Meteorological Institute (Jensen *et al.* 2022; https://www.dmi.dk/publikationer/), from the two stations closest to Steenstrup: Tasiilaq (~180 km SSE) and Aputitieeq (~180km NNE). We calculate the monthly means in 1200 UTC temperatures and present the anomaly from the 1987-2020 average.

5.6.2. Bathymetry

Bathymetric data (fig. S4,5) is derived regionally from the International Bathymetric Chart of the Arctic Ocean (IBCAO) Grid v4.1 (Jakobson *et al.* 2020), and locally from multi-beam echo sounding (MBES) bathymetry data from the Oceans Melting Greenland (OMG) project (OMG, 2019).

Acknowledgements

This project was supported by grants 80NSSC18K1027 and NNX13AI21A from the National Aeronautics and Space Administration. We are grateful to Christine Batchelor for assistance with interpretation of bathymetric data, and to Mike Wood for supplying his sample zones.

Author Contributions

TRC: Conceptualisation, Investigation, Formal analysis, Visualisation, Writing - Original Draft. IMH: Conceptualisation, Investigation, Resources, Funding acquisition, Project administration, Supervision, Writing - Review & Editing. MDK: Investigation, Writing - Review & Editing. AN: Investigation.

Data Availability

Data necessary to replicate this study is available from Zenodo at https://doi.org/10.5281/zenodo.6903790 (Chudley *et al.* 2022). This includes terminus positions, ice discharge history, mélange data, custom ITS_LIVE annual velocity fields, and air and ocean temperature anomaly data. ITS_LIVE scene-pair data are available from https://doi.org/10.5067/IMR9D3PEI28U (Gardner *et al.* 2022). ArcticDEM 2m strips are available at https://doi.org/10.7910/DVN/OHHUKH (Porter *et al.* 2018). The CMEMS Arctic Ocean Physics Reanalysis monthly product is available from https://doi.org/10.48670/moi-00007. Weather station data is available at https://www.dmi.dk/publikationer/ (Jensen *et al.* 2022). BedMachine v4 is available at https://doi.org/10.5067/VLJ5YXKCNGXO (Morlighem *et al.* 2021). IBCAO v4 is available from https://www.gebco.net/ (Jakobsson *et al.* 2020). OMG MBES gridded data is available from https://www.doi.org/10.5067/OMGEV-MBES1 (Oceans Melting Greenland, 2019).

References

Army Map Service (1952). AMS C501 Greenland 1:250,000 Topographic Series - Sheet NQ 25, 26-5 'KJV Steenstrups Søndre Bræ'. Corps of Engineers, U.S. Army, Washington DC. Downloaded from the Polar Geospatial Center https://maps.apps.pgc.umn.edu/id/394

An, L., Rignot, E., Wood, M., Willis, J. K., Mouginot, J., & Khan, S. A. (2021). Ocean melting of the Zachariae Isstrøm and Nioghalvfjerdsfjorden glaciers, northeast Greenland. Proceedings of the National Academy of Sciences, 118(2), e2015483118. https://doi.org/10.1073/pnas.2015483118

Batchelor, C. L., Dowdeswell, J. A., Rignot, E., & Millan, R. (2019). Submarine Moraines in Southeast Greenland Fjords Reveal Contrasting Outlet-Glacier Behavior since the Last Glacial Maximum. Geophysical Research Letters, 46(6), 3279–3286. https://doi.org/10.1029/2019GL082556

Bevan, S. L., Luckman, A. J., Benn, D. I., Cowton, T., & Todd, J. (2019). Impact of warming shelf waters on ice mélange and terminus retreat at a large SE Greenland glacier. The Cryosphere, 13(9), 2303–2315. https://doi.org/10.5194/tc-13-2303-2019

Bindschadler, R., Vornberger, P., Blankenship, D., Scambos, T., & Jacobel, R. (1996). Surface velocity and mass balance of Ice Streams D and E, West Antarctica. Journal of Glaciology, 42(142), 461–475. https://doi.org/10.3189/S0022143000003452

Brough, S., Carr, J. R., Ross, N., & Lea, J. M. (2019). Exceptional retreat of Kangerlussuaq Glacier, east Greenland, between 2016 and 2018. Frontiers in Earth Science, 7, 123. https://doi.org/10.3389/feart.2019.00123

Bunce, C., Carr, J. R., Nienow, P. W., Ross, N., & Killick, R. (2018). Ice front change of marine-terminating outlet glaciers in northwest and southeast Greenland during the 21st century. Journal of Glaciology, 64(246), 523–535. https://doi.org/10.1017/jog.2018.44

Burton, J. C., Amundson, J. M., Cassotto, R., Kuo, C.-C., & Dennin, M. (2018). Quantifying flow and stress in ice mélange, the world's largest granular material. Proceedings of the National Academy of Sciences, 115(20), 5105–5110. https://doi.org/10.1073/pnas.1715136115

Carr, J. R., Stokes, C., & Vieli, A. (2014). Recent retreat of major outlet glaciers on Novaya Zemlya, Russian Arctic, influenced by fjord geometry and sea-ice conditions. Journal of Glaciology, 60(219), 155–170. https://doi.org/10.3189/2014JoG13J122

Carr, J. R., Vieli, A., & Stokes, C. (2013). Influence of sea ice decline, atmospheric warming, and glacier width on marine-terminating outlet glacier behavior in northwest Greenland at seasonal to interannual timescales. Journal of Geophysical Research: Earth Surface, 118(3), 1210–1226. https://doi.org/10.1002/jgrf.20088

Cassotto, R., Fahnestock, M., Amundson, J. M., Truffer, M., & Joughin, I. (2015). Seasonal and interannual variations in ice melange and its impact on terminus stability, Jakobshavn Isbræ, Greenland. Journal of Glaciology, 61(225), 76–88. https://doi.org/10.3189/2015JoG13J235

Cassotto, R., Fahnestock, M., Amundson, J. M., Truffer, M., Boettcher, M. S., Peña, S. D. L., & Howat, I. (2019). Non-linear glacier response to calving events, Jakobshavn Isbræ, Greenland. Journal of Glaciology, 65(249), 39–54. https://doi.org/10.1017/jog.2018.90

Catania, G. A., Stearns, L. A., Moon, T. A., Enderlin, E. M., & Jackson, R. (2020). Future Evolution of Greenland's Marine-Terminating Outlet Glaciers. Journal of Geophysical Research: Earth Surface, 125(n/a), e2018JF004873. https://doi.org/10.1029/2018JF004873

Christian, J. E., Robel, A. A., & Catania, G. (2022). A probabilistic framework for quantifying the role of anthropogenic climate change in marine-terminating glacier retreats. The Cryosphere, 16(7), 2725–2743. https://doi.org/10.5194/tc-16-2725-2022

Chudley, T. R., Howat, I. M., King, M. D., & Negrete, A.. (2022). Data supporting 'Deepwater intrusion triggers sudden and rapid retreat of Greenlandic glacier following long-term stability'. Zenodo. https://doi.org/10.5281/zenodo.6903790

Cooper, M. A., Lewińska, P., Smith, W. A. P., Hancock, E. R., Dowdeswell, J. A., & Rippin, D. M. (2022). Unravelling the long-term, locally heterogenous response of Greenland glaciers observed in archival photography. The Cryosphere, 16(6), 2449–2470. https://doi.org/10.5194/tc-16-2449-2022

Copernicus Marine Environment Monitoring Service (2021), ARCTIC_MULTIYEAR_PHY_002_003, [dataset] https://doi.org/10.48670/moi-00007

van Dongen, E. C. H., Jouvet, G., Sugiyama, S., Podolskiy, E. A., Funk, M., Benn, D. I., et al. (2021). Thinning leads to calving-style changes at Bowdoin Glacier, Greenland. The Cryosphere, 15(2), 485–500. https://doi.org/10.5194/tc-15-485-2021

Enderlin, E. M., Howat, I. M., & Vieli, A. (2013). High sensitivity of tidewater outlet glacier dynamics to shape. The Cryosphere, 7(3), 1007–1015. https://doi.org/10.5194/tc-7-1007-2013

Enderlin, Ellyn M., & Bartholomaus, T. C. (2020). Sharp contrasts in observed and modeled crevasse patterns at Greenland's marine terminating glaciers. The Cryosphere, 14(11), 4121–4133. https://doi.org/10.5194/tc-14-4121-2020

Felikson, D., Bartholomaus, T. C., Catania, G. A., Korsgaard, N. J., Kjær, K. H., Morlighem, M., et al. (2017). Inland thinning on the Greenland ice sheet controlled by outlet glacier geometry. Nature Geoscience, 10(5), 366–369. https://doi.org/10.1038/ngeo2934

Fried, M. J., Catania, G. A., Bartholomaus, T. C., Duncan, D., Davis, M., Stearns, L. A., et al. (2015). Distributed subglacial discharge drives significant submarine melt at a Greenland tidewater glacier. Geophysical Research Letters, 42(21), 9328–9336. https://doi.org/10.1002/2015GL065806

Fried, M. J., Catania, G. A., Stearns, L. A., Sutherland, D. A., Bartholomaus, T. C., Shroyer, E., & Nash, J. (2018). Reconciling Drivers of Seasonal Terminus Advance and Retreat at 13 Central West Greenland Tidewater Glaciers. Journal of Geophysical Research: Earth Surface, 123(7), 1590–1607. https://doi.org/10.1029/2018JF004628

Gardner, A. S., Moholdt, G., Scambos, T., Fahnstock, M., Ligtenberg, S., van den Broeke, M., & Nilsson, J. (2018). Increased West Antarctic and unchanged East Antarctic ice discharge over the last 7 years. The Cryosphere, 12(2), 521–547. https://doi.org/10.5194/tc-12-521-2018

Gardner, A. S., M. A. Fahnestock, and T. A. Scambos. (2022). MEaSUREs ITS_LIVE Landsat Image-Pair Glacier and Ice Sheet Surface Velocities: Version 1, [dataset] https://doi.org/10.5067/IMR9D3PEI28U

Håvik, L., & Våge, K. (2018). Wind-Driven Coastal Upwelling and Downwelling in the Shelfbreak East Greenland Current. Journal of Geophysical Research: Oceans, 123(9), 6106–6115. https://doi.org/10.1029/2018JC014273

Hill, E. A., Carr, J. R., Stokes, C. R., & Gudmundsson, G. H. (2018). Dynamic changes in outlet glaciers in northern Greenland from 1948 to 2015. The Cryosphere, 12(10), 3243–3263. https://doi.org/10.5194/tc-12-3243-2018

Holland, D. M., Thomas, R. H., de Young, B., Ribergaard, M. H., & Lyberth, B. (2008). Acceleration of Jakobshavn Isbræ triggered by warm subsurface ocean waters. Nature Geoscience, 1(10), 659–664. https://doi.org/10.1038/ngeo316

Howat, I. M., Joughin, I., & Scambos, T. A. (2007). Rapid Changes in Ice Discharge from Greenland Outlet Glaciers. Science, 315(5818), 1559–1561. https://doi.org/10.1126/science.1138478

Jackson, R. H., Straneo, F., & Sutherland, D. A. (2014). Externally forced fluctuations in ocean temperature at Greenland glaciers in non-summer months. Nature Geoscience, 7(7), 503–508. https://doi.org/10.1038/ngeo2186

Jakobsson, M., Mayer, L. A., Nilsson, J., Stranne, C., Calder, B., O'Regan, M., et al. (2020). Ryder Glacier in northwest Greenland is shielded from warm Atlantic water by a bathymetric sill. Communications Earth & Environment, 1(1), 1–10. https://doi.org/10.1038/s43247-020-00043-0

Jakobsson, M., Mayer, L. A., Bringensparr, C., Castro, C. F., Mohammad, R., Johnson, P., et al. (2020). The International Bathymetric Chart of the Arctic Ocean Version 4.0. Scientific Data, 7(1), 176. https://doi.org/10.1038/s41597-020-0520-9

Jensen, C. D. (2022) Weather Observations from Greenland 1958-2021 – Observational Data with Description. DMI Report No. 22-08. https://www.dmi.dk/publikationer/

Joughin, I. (2021). MEaSUREs Greenland Monthly Ice Sheet Velocity Mosaics from SAR and Landsat, Version 3. Boulder, Colorado USA. NASA National Snow and Ice Data Center Distributed Active Archive Center. https://doi.org/10.5067/YDLH5QG02XKC

Joughin, I., Shean, D. E., Smith, B. E., & Floricioiu, D. (2020). A decade of variability on Jakobshavn Isbræ: ocean temperatures pace speed through influence on mélange rigidity. The Cryosphere, 14(1), 211–227. https://doi.org/10.5194/tc-14-211-2020

Kehrl, L. M., Joughin, I., Shean, D. E., Floricioiu, D., & Krieger, L. (2017). Seasonal and interannual variabilities in terminus position, glacier velocity, and surface elevation at Helheim and Kangerlussuaq Glaciers from 2008 to 2016. Journal of Geophysical Research: Earth Surface, 122(9), 1635–1652. https://doi.org/10.1002/2016JF004133

Khazendar, A., Fenty, I. G., Carroll, D., Gardner, A., Lee, C. M., Fukumori, I., et al. (2019). Interruption of two decades of Jakobshavn Isbrae acceleration and thinning as regional ocean cools. Nature Geoscience, 12(4), 277–283. https://doi.org/10.1038/s41561-019-0329-3

King, M. D., Howat, I. M., Candela, S. G., Noh, M. J., Jeong, S., Noël, B. P. Y., et al. (2020). Dynamic ice loss from the Greenland Ice Sheet driven by sustained glacier retreat. Communications Earth & Environment, 1(1), 1–7. https://doi.org/10.1038/s43247-020-0001-2

Lea, J. M. (2018). The Google Earth Engine Digitisation Tool (GEEDiT) and the Margin change Quantification Tool (MaQiT) – simple tools for the rapid mapping and quantification of changing Earth surface margins. Earth Surface Dynamics, 6(3), 551–561. https://doi.org/10.5194/esurf-6-551-2018

Liu, J., Enderlin, E., Marshall, H.-P., & Khalil, A. (2022). Synchronous retreat of southeast Greenland's peripheral glaciers. Geophysical Research Letters, n/a(n/a), e2022GL097756. https://doi.org/10.1029/2022GL097756

McFadden, E. M., Howat, I. M., Joughin, I., Smith, B. E., & Ahn, Y. (2011). Changes in the dynamics of marine terminating outlet glaciers in west Greenland (2000–2009). Journal of Geophysical Research: Earth Surface, 116(F2). https://doi.org/10.1029/2010JF001757

Millan, R., Rignot, E., Mouginot, J., Wood, M., Bjørk, A. A., & Morlighem, M. (2018). Vulnerability of Southeast Greenland Glaciers to Warm Atlantic Water From Operation IceBridge and Ocean Melting Greenland Data. Geophysical Research Letters, 45(6), 2688–2696. https://doi.org/10.1002/2017GL076561

Moon, T., Joughin, I., & Smith, B. (2015). Seasonal to multiyear variability of glacier surface velocity, terminus position, and sea ice/ice mélange in northwest Greenland. Journal of Geophysical Research: Earth Surface, 120(5), 818–833. https://doi.org/10.1002/2015JF003494

Morlighem, M., Bondzio, J., Seroussi, H., Rignot, E., Larour, E., Humbert, A., & Rebuffi, S. (2016). Modeling of Store Gletscher's calving dynamics, West Greenland, in response to ocean thermal forcing. Geophysical Research Letters, 43(6), 2659–2666. https://doi.org/10.1002/2016GL067695

Morlighem, M., Williams, C. N., Rignot, E., An, L., Arndt, J. E., Bamber, J. L., et al. (2017). BedMachine v3: Complete Bed Topography and Ocean Bathymetry Mapping of Greenland From Multibeam Echo Sounding Combined With Mass Conservation. Geophysical Research Letters, 44(21), 11,051-11,061. https://doi.org/10.1002/2017GL074954

Morlighem, M., C. Williams, E. Rignot, L. An, J. E. Arndt, J. Bamber, G. Catania, N. Chauché, J. A. Dowdeswell, B. Dorschel, I. Fenty, K. Hogan, I. Howat, A. Hubbard, M. Jakobsson, T. M. Jordan, K. K. Kjeldsen, R. Millan, L. Mayer, J. Mouginot, B. Noël, C. O'Cofaigh, S. J. Palmer, S. Rysgaard, H. Seroussi, M. J. Siegert, P. Slabon, F. Straneo, M. R. van den Broeke, W. Weinrebe, M. Wood, and K. Zinglersen (2021). IceBridge BedMachine Greenland, Version 4. Boulder, Colorado USA. NASA National Snow and Ice Data Center Distributed Active Archive Center. https://doi.org/10.5067/VLJ5YXKCNGXO

Mouginot, J., Rignot, E., Bjørk, A. A., Broeke, M. van den, Millan, R., Morlighem, M., et al. (2019). Forty-six years of Greenland Ice Sheet mass balance from 1972 to 2018. Proceedings of the National Academy of Sciences, 116(19), 9239–9244. https://doi.org/10.1073/pnas.1904242116

Müller, L., Horwath, M., Scheinert, M., Mayer, C., Ebermann, B., Floricioiu, D., et al. (2021). Surges of Harald Moltke Bræ, north-western Greenland: seasonal modulation and initiation at the terminus. The Cryosphere, 15(7), 3355–3375. https://doi.org/10.5194/tc-15-3355-2021

Nuth, C., & Kääb, A. (2011). Co-registration and bias corrections of satellite elevation data sets for quantifying glacier thickness change. The Cryosphere, 5(1), 271–290. https://doi.org/10.5194/tc-5-271-2011

Oceans Melting Greenland. (2019). OMG Swath Gridded Multibeam Echo Sounding (MBES) Bathymetry. Ver. 1. PO.DAAC, CA, USA. https://doi.org/10.5067/OMGEV-MBES1

Porter, C., Morin, P., Howat, I., Noh, M.-J., Bates, B., Peterman, K., et al. (2018). ArcticDEM. Harvard Dataverse. https://doi.org/10.7910/DVN/OHHUKH

Robel, A. A., Pegler, S. S., Catania, G., Felikson, D., & Simkins, L. M. (2022). Ambiguous stability of glaciers at bed peaks. Journal of Glaciology, 1–8. https://doi.org/10.1017/jog.2022.31

Sakakibara, D., & Sugiyama, S. (2018). Ice front and flow speed variations of marine-terminating outlet glaciers along the coast of Prudhoe Land, northwestern Greenland. Journal of Glaciology, 64(244), 300–310. https://doi.org/10.1017/jog.2018.20

Seale, A., Christoffersen, P., Mugford, R. I., & O'Leary, M. (2011). Ocean forcing of the Greenland Ice Sheet: Calving fronts and patterns of retreat identified by automatic satellite monitoring of eastern outlet glaciers. Journal of Geophysical Research: Earth Surface, 116(F3), F03013. https://doi.org/10.1029/2010JF001847

Shepherd, A., Ivins, E., Rignot, E., Smith, B., van den Broeke, M., Velicogna, I., et al. (2020). Mass balance of the Greenland Ice Sheet from 1992 to 2018. Nature, 579(7798), 233–239. https://doi.org/10.1038/s41586-019-1855-2

Slater, D. A., Straneo, F., Das, S. B., Richards, C. G., Wagner, T. J. W., & Nienow, P. W. (2018). Localized Plumes Drive Front-Wide Ocean Melting of A Greenlandic Tidewater Glacier. Geophysical Research Letters, 45(22), 12,350-12,358. https://doi.org/10.1029/2018GL080763

Slater, Donald A., Felikson, D., Straneo, F., Goelzer, H., Little, C. M., Morlighem, M., et al. (2020). Twenty-first century ocean forcing of the Greenland ice sheet for modelling of sea level contribution. The Cryosphere, 14(3), 985–1008. https://doi.org/10.5194/tc-14-985-2020

Snow, T., Straneo, F., Holte, J., Grigsby, S., Abdalati, W., & Scambos, T. (2021). More than Skin Deep: Sea Surface Temperature as a Means of Inferring Atlantic Water Variability on the Southeast Greenland Continental Shelf Near Helheim Glacier. Journal of Geophysical Research: Oceans, 126(4), e2020JC016509. https://doi.org/10.1029/2020JC016509

Straneo, F., & Heimbach, P. (2013). North Atlantic warming and the retreat of Greenland's outlet glaciers. Nature, 504(7478), 36–43. https://doi.org/10.1038/nature12854

Sutherland, D. A., & Pickart, R. S. (2008). The East Greenland Coastal Current: Structure, variability, and forcing. Progress in Oceanography, 78(1), 58–77. https://doi.org/10.1016/j.pocean.2007.09.006

Sutherland, D. A., Straneo, F., Stenson, G. B., Davidson, F. J. M., Hammill, M. O., & Rosing-Asvid, A. (2013). Atlantic water variability on the SE Greenland continental shelf and its relationship to SST and bathymetry. Journal of Geophysical Research: Oceans, 118(2), 847–855. https://doi.org/10.1029/2012JC008354

Todd, J., & Christoffersen, P. (2014). Are seasonal calving dynamics forced by buttressing from ice mélange or undercutting by melting? Outcomes from full-Stokes simulations of Store Glacier, West Greenland. The Cryosphere, 8(6), 2353–2365. https://doi.org/10.5194/tc-8-2353-2014

Todd, Joe, Christoffersen, P., Zwinger, T., Råback, P., Chauché, N., Benn, D., et al. (2018). A Full-Stokes 3D Calving Model applied to a large Greenlandic Glacier. Journal of Geophysical Research: Earth Surface. https://doi.org/10.1002/2017JF004349

Todd, Joe, Christoffersen, P., Zwinger, T., Råback, P., & Benn, D. I. (2019). Sensitivity of a calving glacier to ice—ocean interactions under climate change: new insights from a 3-D full-Stokes model. The Cryosphere. https://doi.org/10.5194/tc-13-1681-2019

Walsh, K. M., Howat, I. M., Ahn, Y., & Enderlin, E. M. (2012). Changes in the marine-terminating glaciers of central east Greenland, 2000–2010. The Cryosphere, 6(1), 211–220. https://doi.org/10.5194/tc-6-211-2012

Walter, F., O'Neel, S., McNamara, D., Pfeffer, W. T., Bassis, J. N., & Fricker, H. A. (2010). Iceberg calving during transition from grounded to floating ice: Columbia Glacier, Alaska. Geophysical Research Letters, 37(15). https://doi.org/10.1029/2010GL043201

Walter, J. I., Box, J. E., Tulaczyk, S., Brodsky, E. E., Howat, I. M., Ahn, Y., & Brown, A. (2012). Oceanic mechanical forcing of a marine-terminating Greenland glacier. Annals of Glaciology, 53(60), 181–192. https://doi.org/10.3189/2012AoG60A083

Williams, J. J., Gourmelen, N., Nienow, P., Bunce, C., & Slater, D. (2021). Helheim Glacier Poised for Dramatic Retreat. Geophysical Research Letters, 48(23), e2021GL094546. https://doi.org/10.1029/2021GL094546

Wood, M., Rignot, E., Fenty, I., Menemenlis, D., Millan, R., Morlighem, M., et al. (2018). Ocean-Induced Melt Triggers Glacier Retreat in Northwest Greenland. Geophysical Research Letters, 45(16), 8334–8342. https://doi.org/10.1029/2018GL078024

Wood, Michael, Rignot, E., Fenty, I., An, L., Bjørk, A., Broeke, M. van den, et al. (2021). Ocean forcing drives glacier retreat in Greenland. Science Advances, 7(1), eaba7282. https://doi.org/10.1126/sciadv.aba7282

Supplement to 'Atlantic Water intrusion triggers rapid retreat and regime change at previously stable Greenland glacier'

Chudley, T. R.[1]*, Howat, I. M.[1,2], King, M. D.[3], Negrete, A.[1]

[1] Byrd Polar and Climate Research Center, Ohio State University, Columbus, OH, USA
[2] School of Earth Sciences, Ohio State University, Columbus, OH, USA
[3] Polar Science Center, University of Washington, Seattle, WA, USA

Correspondence: Tom Chudley (chudley.1@osu.edu)

Supplementary Text

Supplementary Figures 1 – 6

Supplementary Tables 1 – 2

Supplementary Text

BedMachine frontal anomaly at Steenstrup

BedMachine v4 data reports that the front ~600 m of Steenstrup (based on 2016 terminus position) is ~20 m above sea level (fig. 3a), a value that is patently unphysical. We suggest that this is likely due to the fact that OMG MBES data for Steenstrup, which is incorporated into BedMachine (Morlighem *et al.*, 2017), includes the calving face within the bathymetry data (OMG, 2016; fig. S3a), which is thus misinterpreted to become an erroneous sea-level anomaly in synthesised datasets. Manual inspection of the OMG MBES data suggests that the true depth of the calving front lies in the range ~300-360 m, based upon which we suggest the foremost ~1.8 km of the bed profile is unreliable (fig. 3a).

This finding is consistent with Millan et al. (2018), who integrate high-resolution OMG airborne gravimetry data to show that glaciers in SE GrIS have fjords hundreds of metres deeper than shown in BedMachine v3, and fewer shallow sills that limit access to AW. These erroneous data exist even though Steenstrup has a surprising amount of observations for a previously unremarkable glacier, including multiple IceBridge MCoRDS repeats and OMG MBES data. Many other glaciers suffer from a lack of observations entirely. Glaciers with notably long trunks bounded by valleys (typical for the south and central eastern sectors) are poorly represented by BedMachine due to a lack of observational data, with reported thicknesses no greater than tens of metres despite moving at a rates in excess of several metres per day. Named glaciers with these errors include Glacier de France (66.44°N, 35.92°W), Tasilaq Glacier (66.71°N, 34.30°W), and Nordre Parallelgletscher (67.77°N, 33.36°W). It is likely that the current literature, working largely from Greenland-wide synthesis datasets such as BedMachine, has underidentified vulnerable marine-terminating glaciers, with many other previously stable glaciers such as Steenstrup still potentially vulnerable.

References not in main text

OMG (2016). Oceans Melting Greenland Bathymetric Survey - South East Greenland 2016 Operations Report: Appendix A - Daily Field Reports. https://podaac-tools.jpl.nasa.gov/drive/files/allData/omg/L2/docs/2016/Appendix_A-Daily_Reports.pdf

Supplementary Figures

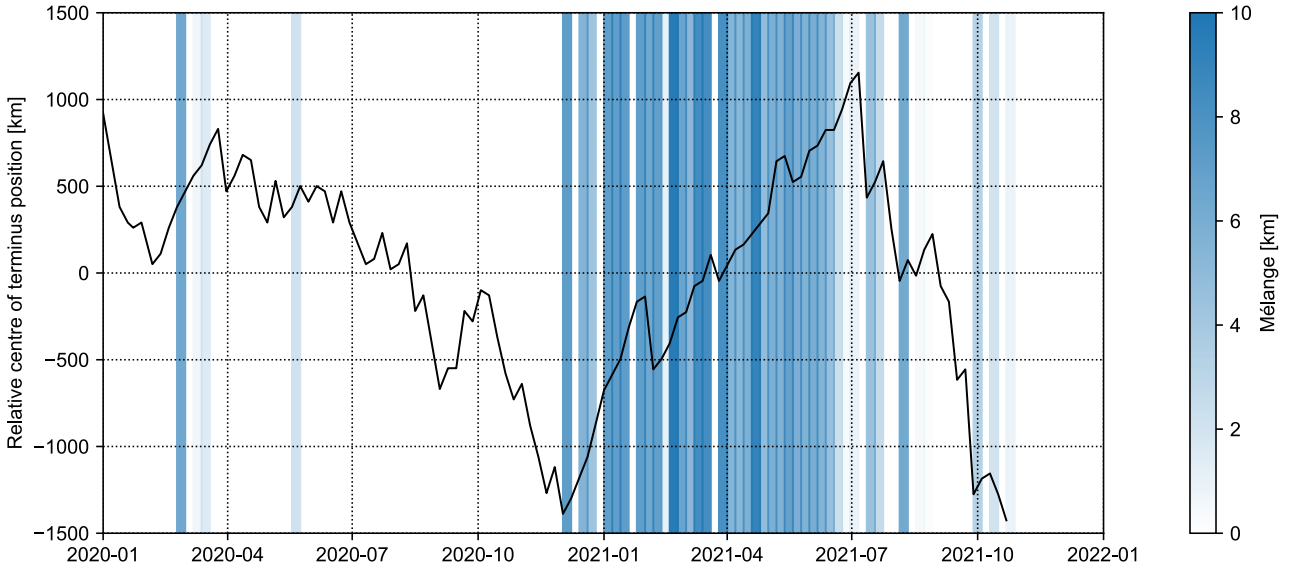

Figure S1: *Enhanced version of fig. 2b showing terminus position (black line) and mélange presence and extent (blue shading) in 2020 and 2021.*

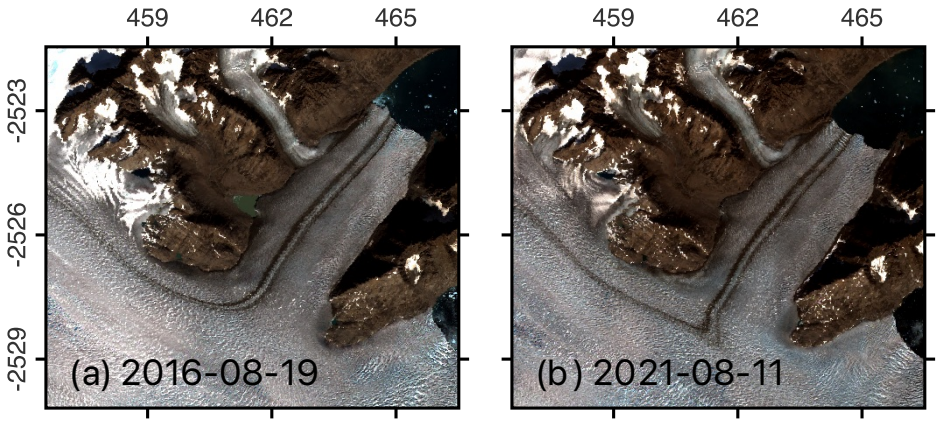

Figure S2: *Sentinel-2 imagery showing displacement of the medial moraine of the northern distributary of Steenstrup between 2016 and 2021 as flow is captured by the main trunk. Coordinates in units km of NSIDC Sea Ice Polar Stereographic North (EPSG:3413).*

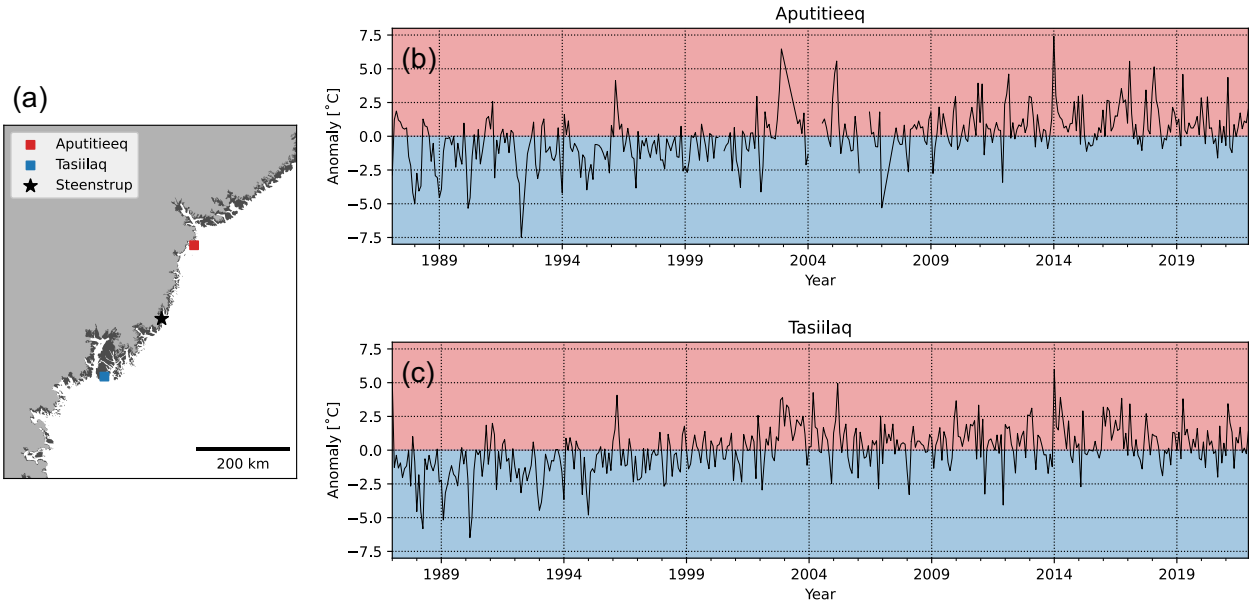

Figure S3: *(a) Location of Aputitieeq and Tasiilaq weather stations relative to Steenstrup. (b) Air temperature anomalies for Aputitieeq. (c) Air temperature anomalies for Tasiilaq.*

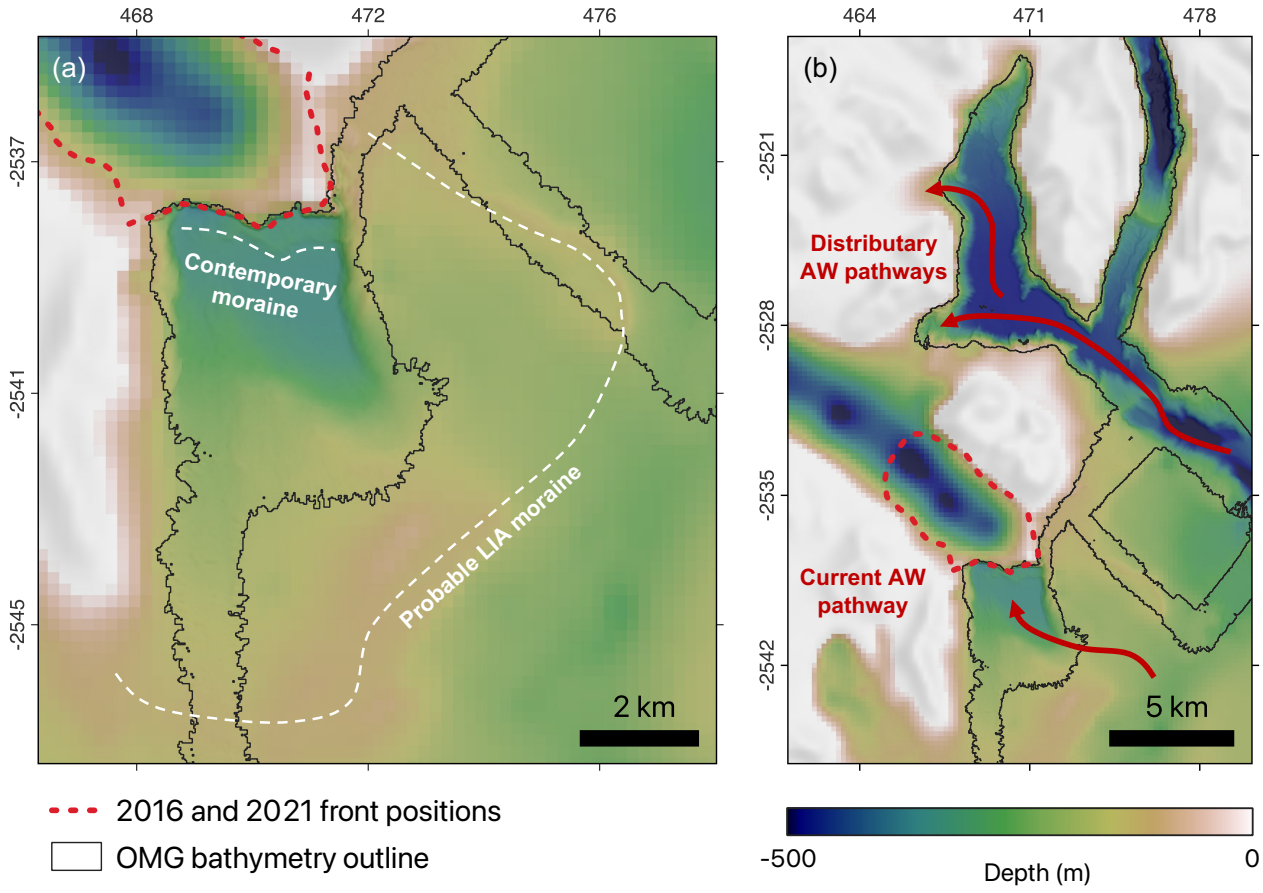

Figure S4: *(a) Hillshaded bathymetric data in front of Steenstrup from IBCAO v4 (which draws subglacial topography from BedMachine) and OMG MBES data. White dashed lines mark the contemporary and Little Ice Age (LIA) moraines identified by Batchelor* et al. *(2019). NB the artificial sea-level topography introduced into BedMachine at the 2016 terminus position due to OMG MBES incorporation of the calving front. (b) Potential alternative AW pathways through the distributaries. NB the inability of BedMachine to resolve ice depth at the northern distributary.*

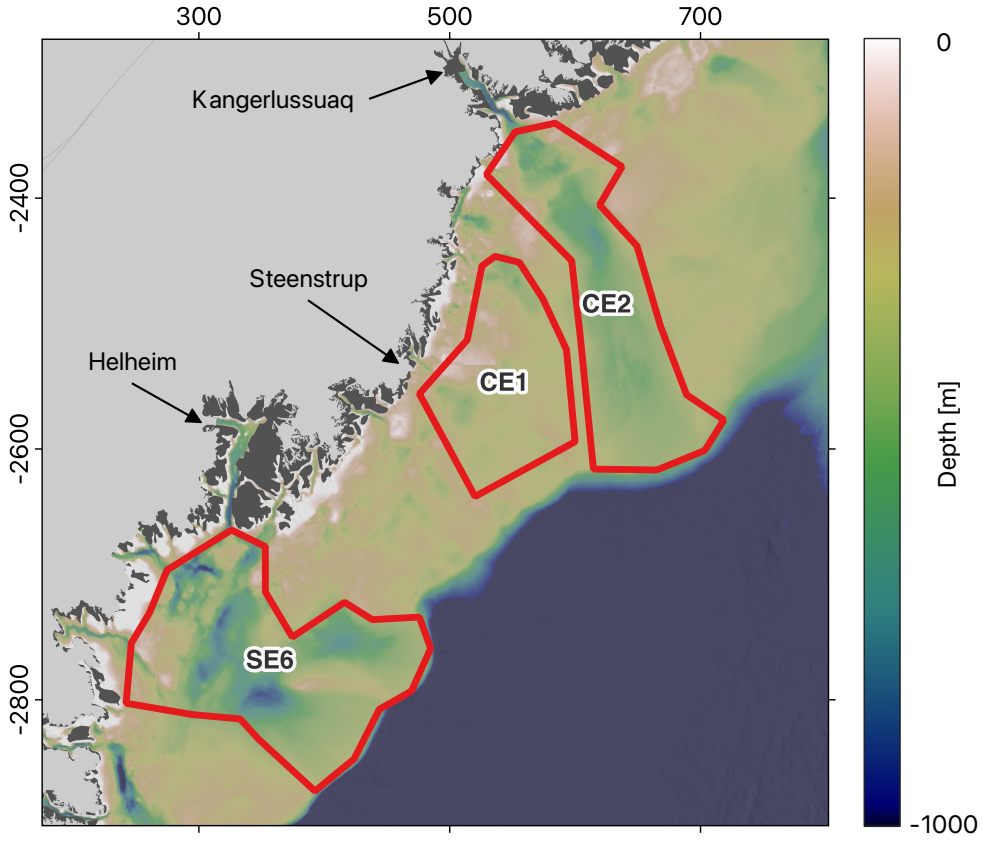

Figure S5: *Location of Wood* et al. *(2021) sample zones. Background is hillshaded IBCAO bathymetry. Coordinates are in units km of NSIDC Sea Ice Polar Stereographic North (EPSG:3413).*

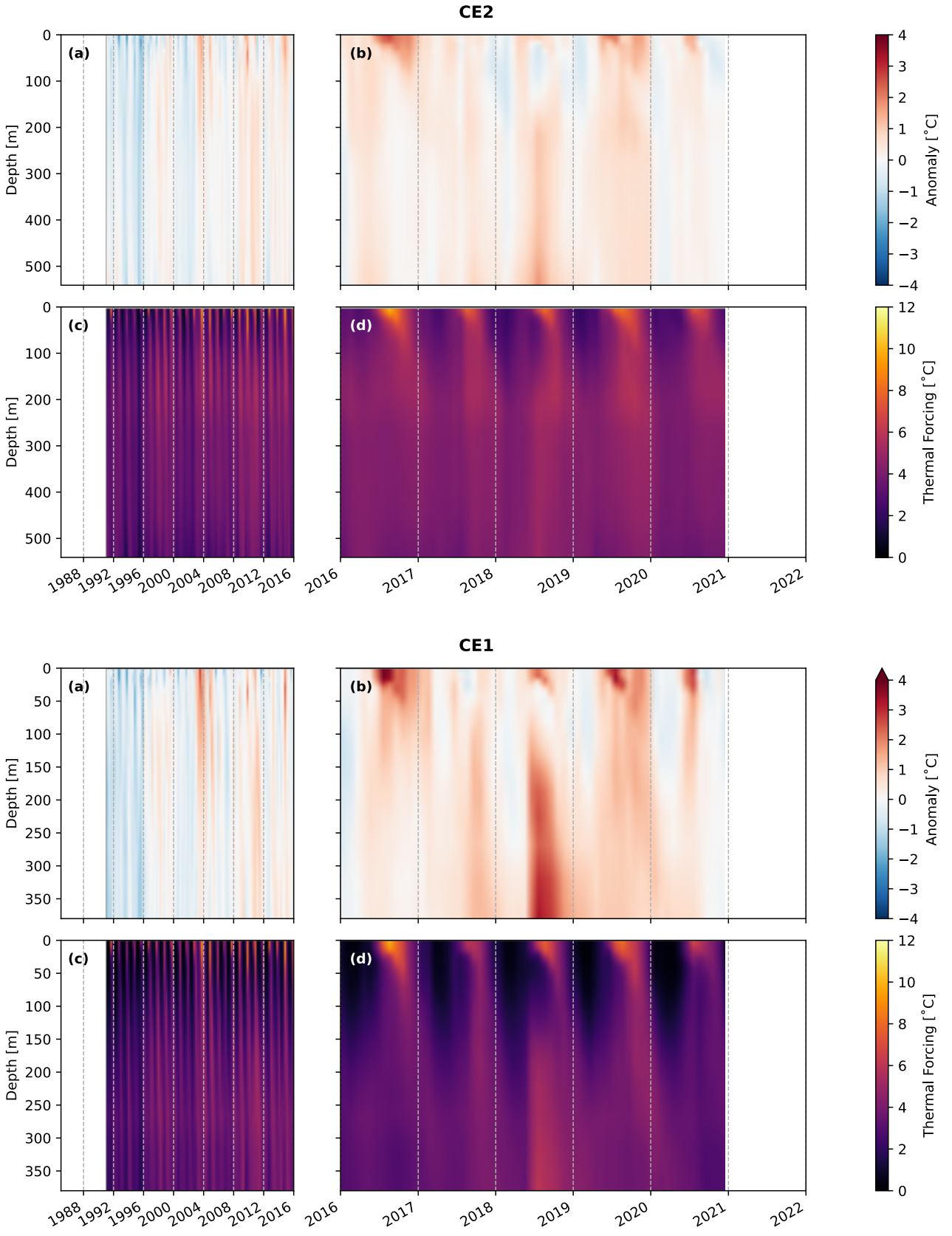

Figure S6: *Ocean temperature anomaly and thermal forcing for each of the CE2, CE1, and SE6 sample zones from Wood* et al. *(2021). For each subfigure: (a) Temperature anomaly from the 1992-2021 mean between 1992 and 2015. (b) Temperature anomaly from the 1992-2021 mean between 2016 and 2021. (c) Thermal forcing between 1992 and 2015. (d) Thermal forcing between 2016 and 2021.* ***(continues on next page)***

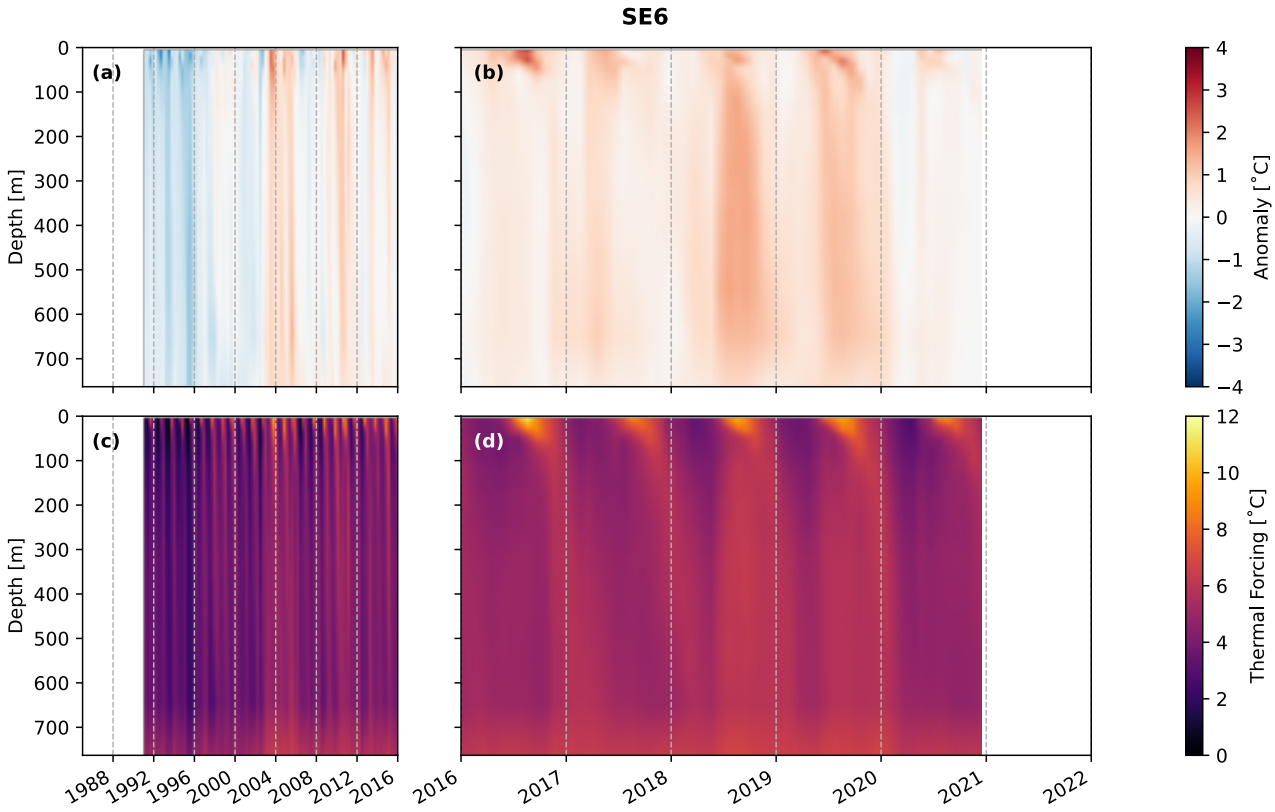

Figure S6: *(continued)*

Supplementary Tables

Table S1: *Positions of sampling points presented in Fig 1a and Fig 2b, in coordinates of NSIDC Sea Ice Polar Stereographic North (EPSG:3413).*

Point	**X**	**Y**
a	464895	-2533001
b	460732	-2530257
c	456475	-2527582
d	451777	-2526768

Table S2: *Date and IDs of ArcticDEM strips used*

Date	**ArcticDEM 2m Strip**
2016-03-27	WV01_20160327_102001004BC7AC00_102001004AC12E00_2m_lsf
2016-04-04	WV01_20160404_102001004AA8F800_102001004D67D900_2m_lsf
2016-08-03	WV01_20160803_1020010054389200_10200100537DE100_2m_lsf
2017-06-07	WV01_20170607_1020010063D4CE00_10200100617E7F00_2m_lsf
2017-08-05	WV01_20170805_1020010065C0F200_102001006260ED00_2m_lsf
2018-04-05	WV01_20180405_1020010072328700_102001007149E600_2m_lsf
2018-04-23	WV03_20180423_104001003A7FE400_104001003A9F3100_2m_lsf
2018-05-30	WV03_20180530_104001003DC69400_104001003E486E00_2m_lsf
2019-05-11	WV03_20190511_104001004BBA4500_104001004C5DCC00_2m_lsf
2019-06-14	WV01_20190614_102001008B302C00_1020010087237C00_2m_lsf
2019-07-22	WV01_20190722_1020010086AC6800_1020010085418C00_2m_lsf
2020-07-09	WV01_20200709_102001009A689B00_102001009B63B200_2m_lsf
2020-07-14	WV01_20200714_102001009BEB8300_102001009CB09500_2m_lsf
2021-07-31	WV02_20210731_10300100C359CF00_10300100C37C8000_2m_lsf
2021-08-14	WV02_20210814_10300100C3611400_10300100C4831700_2m_lsf